4. Chemistry of Borehole Fluids Collected at PACMANUS, Papua New Guinea, ODP Leg 193[1]

R.A. Binns,[2, 3] L.E. Dotter,[2] and K.A. Blacklock[4]

ABSTRACT

Four samples of borehole fluid collected with the Water Sampling Temperature Probe at the PACMANUS hydrothermal during Leg 193 were all significantly diluted by entrained seawater, and one also contained residual deionized water from the tool. The least contaminated sample (88% seawater) was collected 130 meters below seafloor in Hole 1189B, at a temperature of 55°C. Its trace element and strontium isotope constitution indicate the presence of a hydrothermal component similar to high-temperature fluids vented from seafloor sulfide chimneys at PACMANUS, plus excess $CaSO_4$ dissolved from wallrock anhydrite. A fluid collected at 6°C close to the seafloor in Hole 1188B has ~2% of a less well defined hydrothermal component mixed with $CaSO_4$ dissolved from wallrock anhydrite deeper in the hole. It has anomalously high Mn, Zn, and Mo contents. Unlike the Hole 1189B sample and two more highly diluted samples from Hole 1188F, its Mn/Fe ratio lies well outside the constrained range measured previously at PACMANUS for chimney vent fluids, plume particulates, and diffusely vented fluids collected above the seafloor by funnel. Uncertainties associated with these results demonstrate that improved technology is desirable for sampling high-temperature fluids during future drilling at oceanic hydrothermal sites.

[2]Division of Exploration and Mining, Commonwealth Scientific and Industrial Research Organisation (CSIRO), PO Box 136, North Ryde NSW 1670, Australia. Correspondence author: Ray.Binns@csiro.au
[3]Department of Earth Marine Sciences, Australian National University, Canberra ACT 0200, Australia.
[4]Division of Petroleum Resources, Commonwealth Scientific and Industrial Research Organisation (CSIRO), PO Box 136, North Ryde NSW 1670, Australia.

INTRODUCTION

Significant chemical differences have been recognized in recent years between hydrothermal vent fluids associated with actively forming sulfide chimneys at mid-ocean ridges (Von Damm, 1995) and backarc basin submarine volcanic sites including PACMANUS in the Manus Basin of northern Papua New Guinea (Binns and Scott, 1993; Gammo et al., 1996; Douville et al., 1999). In order to further understand these differences, particularly the role of subseafloor reactions with contrasted mafic and felsic substrates and possible contributions from introduced magmatic components, sampling deep-seated borehole fluids for comparison with those vented from active seafloor chimneys at PACMANUS was an important although poorly achieved objective of Leg 193. Our intention to develop a tool capable of handling anticipated high temperatures to 350°C being unrealized, we used the Water Sampling Temperature Probe (WSTP) (Barnes, 1988) previously employed by the Ocean Drilling Program (ODP) to collect in situ pore fluids from sediments.

Four borehole fluid samples were collected during the leg. Details of the operations and shipboard chemical analyses are provided in Binns, Barriga, Miller, et al. (2002) and are summarized in Table T1. To avoid damage to the tool, we conservatively planned to lower the WSTP to depths where prior logging runs indicated a borehole temperature of 60°C, timing the opening of its valve accordingly. This plan was frustrated in Hole 1188B by a blockage close to the seafloor, at which point faulty operation of the inlet valve also apparently prevented complete flushing of deionized water from the sampling coil. Two samples obtained at different times in Hole 1188F were collected at lower than expected temperatures as a consequence of seawater draw-down into the hole. Only the sample from Hole 1189B was collected at a temperature close to the objective (55°C), although premature opening of the valve during this operation may have trapped some fluid from higher in the hole.

Shipboard analyses (Binns, Barriga, Miller, et al., 2002) established that all four borehole fluid samples were composed principally of seawater. Elevated Fe, Mn, and Li in the more successful sample from Hole 1189B suggested a hydrothermal component, whereas Mn was also enriched in the near-seabed sample from Hole 1188B. High Ca in the sample from Hole 1189B was interpreted to possibly arise from anhydrite dissolution.

This report presents shore-based chemical and Sr isotopic analyses of subsamples from each operation, taken from the titanium primary sampling coil of the WSTP, filtered through 0.2-µm polysulfone membranes, and acidified with 0.1 mL of ultrapure HNO_3 per 10 mL of sample. Three blank samples, prepared on board from similarly acidified nanopure water, were also analyzed.

Details of the tectonic setting, volcanology, and sub-seafloor alteration patterns of the PACMANUS hydrothermal field, located along the crest of felsic volcanic Pual Ridge, are provided by the Shipboard Scientific Party (2002a) and elsewhere in this volume. Key points warranting mention here are that Pual Ridge is constructed of relatively thin flows, predominantly dacite and rhyodacite with some andesite, and that at the sites drilled the sequence is pervasively altered to clay-dominated assemblages beneath a thin cap (<10–40 m) of unaltered volcanic rock. Borehole fluids were collected at two sites: Site 1188, located on a zone

of low-temperature, diffuse venting (Snowcap site, drilled to 387 meters below seafloor [mbsf] with Hole 1188F), and Site 1189, located at a field of active sulfide chimneys with high-temperature, focused venting (Roman Ruins Site, drilled to 206 mbsf with Hole 1189B). The settings of these and other named sites referred to below are shown in Figure F1.

METHODS

Chemical analyses (Table T1) were performed by inductively coupled plasma–atomic emission spectrometry (ICP-AES) at Commonwealth Scientific and Industrial Research Organisation (CSIRO), Sydney, Australia, and by inductively coupled plasma–mass spectrometry (ICP-MS) at University of Technology, Sydney, Australia, using Spectroflame and PerkinElmer instruments, respectively. For ICP-AES measurements, conducted in duplicate, the borehole fluids and shipboard blank samples were introduced undiluted and at various dilutions to optimize the concentration range and minimize corrections for spectral overlaps and suppressive interferences. Aqueous calibration standards were used, and instrumental blanks were computed using ultrapure deionized water.

Measurements by ICP-MS were conducted twice on different days with similar results and, for the borehole samples, a third time under conditions providing increased sensitivity, particularly for rare earth elements (REE). The shipboard blank samples were run undiluted, whereas borehole fluids were diluted ×30 to help minimize interferences (which nevertheless prevented determination of Sc, V, Cu, and As by this method). Calibration and blank solutions were prepared from ultrapure deionized water and were acidified to a pH equivalent to that of the samples. Internal reference spikes (Re and Rh) were added to samples and calibration solutions.

Detection limits based on count statistics and respective dilutions are listed in Table T1. These are considered variously conservative, and some analyses below the nominal detection limits are cited as meaningful. Data are not provided where our prior experience with saline groundwaters indicates that the use of matrix-unmatched aqueous standards is not appropriate for analysis of seawater.

For strontium isotope measurements, Sr was separated directly from the borehole fluids by cation exchange chromatography with AG50W-X8 resin and loaded with H_3PO_4 onto Ta filaments. Isotope ratios were measured on a VG 354 thermal ionization mass spectrometer at CSIRO. Measured blanks were negligible. Raw data from 54 ratio determinations were filtered using a 2σ rejection criterion. Internal precisions calculated as two standard errors of the mean are cited in Table T1. Twelve simultaneous ratio measurements of the U.S. National Bureau of Standards Standard Reference Material 987 standard averaged 0.710231 (2σ = 0.0023%).

Chemical analyses of other CSIRO samples used in comparative discussions below were obtained using the same methods. These include a filtered vent fluid collected at a Tsukushi chimney in 1998 by C.J. Yeats (BIOACCESS cruise, *Shinkai-2000* Dive 1066), samples from within the particulate plume above PACMANUS collected in standard Niskin bottles during hydrocasts at three sites between the Satanic Mills and Roman Ruins chimney fields (BINATANG and BISMARCK cruises of the *Franklin* in 2000 and 2002, respectively, and the DaeYang-02 cruise of the *Onnuri* in 2002; unpublished CSIRO reports) and vent funnel (VUNL) samples from three warm seeps on the diffusely venting Snow-

R.A. Binns et al.
Chemistry of Borehole Fluids

4
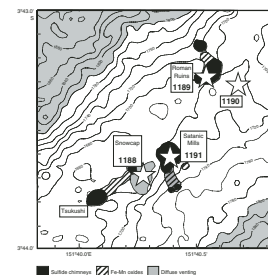
cap field (PACMANUS-IV and BINATANG cruises of *Franklin* in 1997 and 2002, respectively; unpublished CSIRO reports). The VUNLs were inverted tetragonal prisms, 1.5 m across on their open base and with narrow openings at the top, constructed of stainless steel (mild steel lined with plastic in the first version), and fitted with an altimeter, a temperature sensor, and a small Niskin bottle. With favorable weather conditions, the VUNL was moved around and gently "pogoed" to bottom until a temperature anomaly was noted, at which point the Niskin bottle was triggered after allowing 15–20 min to stabilize. Temperatures during collection ranged from 0.1° to 0.5°C above ambient.

RESULTS

Analyses of the shipboard blank samples (Table T1) were below or close to detection limits for most elements. Minor traces of Ni, Zn, Rb, Sr, Y, Mo, Cd, Sb, REE, Pb, and Bi were measured. In no case did the level require application of a correction for the acid spike to those borehole fluids where presence of a hydrothermal component is apparent.

Allowing a density of 1.025 g/mL for seawater, agreement between the shore-based analyses (here cited gravimetrically) and shipboard analyses (cited volumetrically by Binns, Barriga, Miller, et al., 2002) of the borehole fluids is excellent for Na, Mg, and S and good for K, Ca, B, Sr, and Li. However, the new results for Mn, Fe, and Ba are distinctly lower.

The compositions and $^{87}Sr/^{86}Sr$ ratios of the two borehole samples from 107 and 207 mbsf in Hole 1188F (CSIRO numbers 142725 and 142726) are essentially identical with seawater, except for modest enrichments in Mn, Fe, Co, Zn, Cd, light REE, Pb, Bi, and Th—elements (apart from Th) conceivably contributed by a tiny proportion of hydrothermal fluid (≤1%). The lower Na, Mg, and S contents cited here, as well as the shipboard salinity measurement and Cl analysis (506 mMol/L) for the borehole sample at 3 mbsf in Hole 1188B (CSIRO 142724) indicate that some deionized water remained in the WSTP coil. Using Na and Cl contents as a guide, both elements of comparable abundance in both seawater and hydrothermal fluids, the dilution is estimated at 8%. This near-seabed sample and also the higher-temperature borehole fluid from 130 mbsf in Hole 1189B (CSIRO 142727) display a number of elemental enrichments potentially attributable to hydrothermal components, which we assessed by applying corrections for entrained seawater (Table T2). Both also show significantly lower bulk $^{87}Sr/^{86}Sr$ ratios than seawater (Table T1).

The composition used for seawater (Table T2) is based on four hydrocast samples, analyzed using the same methods, all collected near 1500 meters below sea level (mbsl) over Pual Ridge, northeast of PACMANUS, from background positions outside the detectable particulate plume. This seawater composition differs significantly from literature values only by its higher Pb, an element that appears to have been dispersed beyond the particulate plume at PACMANUS, but for which any adjustment makes no relevant change to our end-member calculations. Literature values were used for the REE (Mitra et al., 1994) because like Ga, Ge, As, and Te these were below detection by ICP-MS in the Pual Ridge background seawaters.

The proportions of seawater in borehole samples from 3 mbsf in Hole 1188B (CSIRO 142724) and from 130 mbsf in Hole 1189B (CSIRO 142727) were assessed by assuming this component contained all the

bulk Mg and that hydrothermal fluids contain zero Mg (see Von Damm, 1995). Taking into account also the estimated deionized water dilution in the former, their calculated hydrothermal end-member components (Mg = 0) are 2% and 12%, respectively, the first figure being subject to greater error. End-member compositions computed by subtracting seawater contributions and recalculating to 100% are presented in Table T2 for elements adequately detected. The calculations yield negative end-member values for U, reflecting lower contents than seawater in the raw analyses of these two samples. We are especially confident regarding the latter, so an additional extractive factor discussed below appears involved.

Table T2 also lists, for comparison, similar calculations applied to analyses (Douville, 1999) of fluids collected by the *Shinkai-6500* from two chimney vents at Satanic Mills (Fig. F1) during the 1995 ManusFlux cruise (Auzende et al., 1996). Bach et al. (2004) argue the case for using Mg = 0 to calculate these PACMANUS end-members, rather than Mg = 20 mM as proposed by Douville et al. (1999). For many elements including the alkalis, the calculated end-member composition for the 55°C borehole fluid at 130 mbsf in Hole 1189B (CSIRO 142727) falls within or close to the range of the chimney vent fluid end-members. In comparison with the vent fluids, highly enriched elements in the borehole fluid include total S, Ca, Cd, and REE; moderately enriched elements include Sr and Sb; and depleted elements include Al, Mn, Fe, Mo, and Pb.

Although subject to greater error arising from the estimated dilution by deionized water, the calculated end-member for near-seabed borehole fluid at 3 mbsf in Hole 1188B (CSIRO 142724) is broadly similar that of the sample from 130 mbsf in Hole 1189B (CSIRO 142727), but Mn, Zn, Mo, Cd, Sb, and La are distinctly higher, whereas K and Fe are lower. In addition, Co, Ni, and Th are higher, but no data are available for these elements in the chimney vent fluids.

A chondrite-normalized REE plot (Fig. F2) for end-member fluid from 130 mbsf in Hole 1189B (CSIRO 142727) shows progressive relative depletion in heavy REE but lacks any significant Eu anomaly. In both this and the overall increased REE abundances, this end-member composition differs significantly from the end-member chimney vent fluids at Satanic Mills, which are comparatively depleted in light REE and have distinctly positive Eu anomalies (Fig. F2). Douville et al. (1999) attribute depletion of light REE in the vent fluids to subsurface precipitation of barite. This mineral is conspicuously rare in Leg 193 drill core from below Roman Ruins and Snowcap, but Satanic Mills remains untested in that respect because Hole 1191A at that site did not penetrate beyond a >20 m capping of unaltered dacite.

The partial end-member REE plot (Fig. F2) for the borehole fluid from 3 mbsf in Hole 1188B (CSIRO 142724) shows highly enriched La and a negative Ce anomaly. Raw values for La and Ce for the two borehole fluids from 107 and 207 mbsf in Hole 1188F (CSIRO 142725 and 142726) (Table T1) are higher than seawater, and the ratios suggest they share a negative Ce anomaly.

Using the proportions of seawater and apparent hydrothermal end-member, their measured bulk $^{87}Sr/^{86}Sr$, and the original and computed end-member contents of Sr, we estimated $^{87}Sr/^{86}Sr$ for the end-member component of borehole fluids at 3 mbsf in Hole 1188B (CSIRO 142724) and 130 mbsf in Hole 1189B (CSIRO 142727) and also of the chimney vent fluids (Table T2). The borehole fluid end-member ratios are comparable (0.7064 and 0.7062), but they are more radiogenic than those of

F2. Chondrite-normalized REE profiles, p. 11.
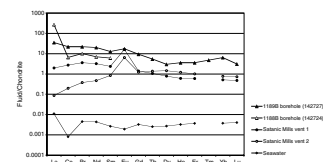
the chimney vent fluids (0.7050 and 0.7054). The former fall within the range measured for vein anhydrite from deeper cores at Sites 1188 and 1189 (Roberts et al., 2003); anhydrites closer to the seabed have ratios nearer seawater. All four borehole and chimney end-member ratios are higher than unaltered lavas dredged from Pual Ridge (0.70359; $n = 13$) and an altered dacite cropping out at Snowcap (0.70470) (CSIRO data).

DISCUSSION

Any genuine hydrothermal fluid passing out of fracture conduits will be principally mixed within the Leg 193 boreholes by remnant drilling fluid (surface seawater) and near-seabed seawater drawn into the holes after drilling or already added by circulation deeper within the PAC-MANUS hydrothermal system. Our end-member calculations treat these as a single component. Other sources of contamination include material leached from wallrocks by the borehole fluid and material dissolved from sepiolite or barite muds used to flush the holes. Leaching of Mg from sepiolite would affect our estimates of seawater components but cannot be evaluated, although we assume the effect is negligible. Low Ba contents of the samples preclude significant contamination by barite.

The high Ca contents calculated for the end-member borehole fluids, around 6 or 7 times those of the end-member chimney vent fluids, suggest there has been some leaching of anhydrite from wallrock veins and breccias at the measured temperatures of collection. This would also contribute S and Sr to the borehole fluids. The apparent excess of S in the two more successful end-member borehole fluids (confirmed as sulfate by shipboard analyses and the lack of H_2S odor), relative to total S (SO_4^{2-} and H_2S) in the end-member chimney vent fluids, is indeed only slightly below the stoichiometric equivalent of Ca in anhydrite. Trace Sr in Leg 193 anhydrites varies from 207 to 4568 ppm, averaging 2630 ppm for 59 samples (Roberts et al., 2003). To explain the excess Sr in the two end-member borehole fluids this way would require dissolution of anhydrite containing 1000–1400 ppm Sr, well within the measured range.

The $^{87}Sr/^{86}Sr$ ratios measured on vein anhydrites at Sites 1188 and 1189 together with depth profiles implying higher degrees of seawater mixing for anhydrite-crystallizing fluids close to the seafloor (Roberts et al., 2003) allow further inferences if indeed anhydrite dissolution has contributed to the borehole fluids. The calculated end-member $^{87}Sr/^{86}Sr$ (0.7062) for the borehole fluid sampled at 130 mbsf in Hole 1189B (CSIRO 142727) is close to the average value of 0.7065 measured in vein anhydrites from 118 to 158 mbsf within the lower sequence (Shipboard Scientific Party, 2002b) of Hole 1189B. While this might be coincidental considering anhydrite variability in this interval ($^{87}Sr/^{86}Sr$ σ = 0.0006; n = 16), it hints that more than just the excess Ca and Sr could have dissolved from anhydrite. For the sample collected at 3 mbsf in Hole 1188B (CSIRO 142724), however, the end-member $^{87}Sr/^{86}Sr$ estimate (0.7064) is distinctly lower than the ratios in anhydrites collected from the upper 50 m of nearby Hole 1189A (average = 0.7078; σ = 0.0009; n = 6), but closer to ratios for anhydrites below 50 mbsf in Holes 1188A and 1188F (average = 0.7061; σ = 0.0005; n = 51). This strongly suggests that borehole fluid sampled near the seabed in Hole 1188B was ascending from far greater depths.

The REE abundances and chondrite-normalized patterns of anhydrites from Sites 1188 and 1189 are extremely variable (Bach et al., 2004). Concentrations of Nd range from 0.08 to 28.3 ppm, and the patterns include light-REE enrichment and depletion or mid-REE enrichment and depletion, with some negative but mostly positive Eu anomalies. Again using apparent excess Ca, even the maximum Nd measured in anhydrite would contribute only 0.24–0.30 ppm Nd if dissolved into the end-member borehole fluids, distinctly below their computed concentrations of this element (Table T2). The abundances and chondrite-normalized patterns of REE in the borehole fluids, relative to chimney vent fluids, remain unexplained. Leaching from altered wallrocks is unlikely since these mostly show pronounced Eu depletion (see Fig. F19B in Binns, this volume [Manuscript 211]).

Aside from the anhydrite dissolution and REE issues, the computed end-member composition of the borehole fluid sampled at 130 mbsf in Hole 1189B (CSIRO 142727; Roman Ruins) is remarkably similar to those of the end-member vent fluids from Satanic Mills chimneys for most elements, exceptions being its lower Al, somewhat lower Fe and Mg, and, among the chalcophile elements, higher Cd and lower Mo and Pb. Contents of Cu and Zn are similar. The general resemblance suggests that the hydrothermal component within the borehole fluid is dominated by a substantial portion of vent-type fluid. However, the lack of H_2S in the former requires there to have been some oxidation of the latter. The particularly low U content of the original borehole fluid relative to seawater indicates this element has been extracted from its hydrothermal component. Although U is normally mobile under oxidized conditions and deposited by reduction to UO_2, this element is relatively abundant in low-temperature Fe-Mn-Si oxide deposits at PACMANUS (see Table T2 in Binns, this volume [Manuscript 211]), possibly as a result of adsorptive scavenging. Postdrilling oxidation and deposition of oxides within or near the borehole might cause lower Fe, Mn, and U contents in the collected sample.

Similarity of the "hydrothermal" component to chimney vent fluids is less evident for the sample from 3 mbsf in Hole 1188B (CSIRO 142724). As calculated, with inherent errors arising from the effect of dilution by deionized water on the estimated hydrothermal component, it is exceptionally rich in Mn, Zn, Mo, Cd, Sb, and La; depleted in K, Fe, and Pb; and again deficient in U. Some of these characteristics, as well as negative Ce anomalies, are shared by Mn-rich oxide deposits dredged at and near Snowcap (Site 1188), to which the Hole 1188B borehole fluid may have a greater affinity than sulfide chimneys, as a consequence of subsurface reactions that can not at present be quantified.

The Mn/Fe ratio in the borehole fluid sampled at 3 mbsf in Hole 1188B (CSIRO 142724) is exceptional. Figure F3 plots abundance of these elements in end-member components for two sets of samples from vents 1 and 2 at Satanic Mills (Douville, 1999; Gamo et al., 1996; T. Gamo, pers. comm., 1996), together with samples (more diluted by seawater) collected at a third Satanic Mills chimney and one at Roman Ruins (Gammo et al., 1996; T. Gammo, pers. comm., 1996), plus a sample from a Tsukushi chimney (C.J. Yeats, pers. comm., 2001). All these show limited variation in Mn/Fe ratio, although the Tsukushi composition is somewhat richer in Fe. Also plotted in Figure F3, without extrapolation to zero Mg, are total dissolvable Mn and Fe in samples collected by VUNL at Snowcap warm seeps and by hydrocast from the "eye" of the particulate plume directly above PACMANUS. These latter are

F3. Logarithmic plot of Fe and Mn contents, p. 12.
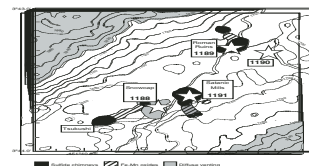
highly diluted by seawater but are considered, respectively, to reflect the Mn/Fe ratios in diffusely vented fluids at Snowcap and the residue of chimney fluids vented at Satanic Mills and Roman Ruins. They possess Mn/Fe ratios comparable with the chimney vent fluids, as do the highly diluted borehole fluids collected at 107 and 207 mbsf in Hole 1188F (CSIRO 142725 and 142726). The near-seabed borehole sample from 3 mbsf in Hole 1188B (CSIRO 142724) falls well off the general trend.

The above discussion is clearly based on imperfect samples of borehole fluids from PACMANUS and on perhaps ambitious extrapolation from analytical data for the raw samples. The results provide additional information requiring consideration in overall interpretations of the PACMANUS hydrothermal system, but they do not permit quantitative assessments regarding subseafloor fluid-rock interactions or input of magmatic fluids, as we hoped prior to conducting Leg 193. They establish a need to develop improved technology for collecting higher-temperature fluids during future ocean drilling focused on submarine hydrothermal systems.

ACKNOWLEDGMENTS

REFERENCES

Auzende, J.-M., Urabe, T., and Scientific Party, 1996. Cruise explores hydrothermal vents of the Manus Basin. *Eos, Trans. Am. Geophys. Union,* 77:244.

Bach, W., Roberts, S.R., Vanko, D.A., Binns, R.A., Yeats, C.J., Craddock, P.R., and Humphris, S.E., 2004. Controls of fluid chemistry and complexation on rare earth element contents of anhydrite from the PACMANUS subseafloor hydrothermal system, Manus Basin, Papua New Guinea. *Miner. Deposita,* 38:916–935.

Barnes, R.O., 1988. ODP in-situ fluid sampling and measurement: a new wireline tool. *In* Mascle, A., Moore, J.C., et al., *Proc. ODP, Init. Repts.,* 110: College Station, TX (Ocean Drilling Program), 55–63.

Binns, R.A., Barriga, F.J.A.S., Miller, D.J., et al., 2002. *Proc. ODP, Init. Repts.,* 193 [CD-ROM]. Available from: Ocean Drilling Program, Texas A&M University, College Station TX 77845-9547, USA.

Binns, R.A., and Scott, S.D., 1993. Actively forming polymetallic sulfide deposits associated with felsic volcanic rocks in the eastern Manus back-arc basin, Papua New Guinea. *Econ. Geol.,* 88:2226–2236.

Douville, E. 1999. Les fluides hydrothermaux oceaniques comportement geochimique des elements traces et des terres rares: Processus associes et modelisation thermodynamique [PhD Thesis]. Univ. Brest, France.

Douville, E., Bienvenu, P., Charlou, J.L., Donval, J.P., Fouquet, Y., Appriou, P., and Gamo, T., 1999. Yttrium and rare earth elements in fluids from various deep-sea hydrothermal systems. *Geochim. Cosmochim. Acta,* 63:627–643.

Gamo, T., Okamura, K., Kodama, Y., Charlou, J.-L., Urabe, T., Auzende, J.-M., Shipboard Scientific Party of the ManusFlux Cruise, and Ishibashi, J., 1996. Chemical characteristics of hydrothermal fluids from the Manus back-arc basin, Papua New Guinea. I. Major chemical components. *Eos, Trans. Am. Geophys. Union,* 77 (Suppl.):W116.

Mitra, A., Elderfield, H., and Greaves, M.J., 1994. Rare earth elements in submarine hydrothermal fluids and plumes from the Mid-Atlantic Ridge. *Mar. Chem.,* 46:217–235.

Roberts, S., Bach, W., Binns, R.A., Vanko, D.A., Yeats, C.J., Teagle, D.A.H., Blacklock, K., Blusztajn, J.S., Boyce, A.J., Cooper, M.J., Holland, N., and McDonald, B., 2003. Contrasting evolution of hydrothermal fluids in the PACMANUS system, Manus Basin; the Sr and S isotope evidence. *Geology,* 31:805–808.

Shipboard Scientific Party, 2002a. Leg 193 summary. *In* Binns, R.A., Barriga, F.J.A.S., Miller, D.J., et al., *Proc. ODP, Init. Repts.,* 193: College Station TX (Ocean Drilling Program), 1–84.

Shipboard Scientific Party, 2002b. Site 1189. *In* Binns, R.A., Barriga, F.J.A.S., Miller, D.J., et al., *Proc. ODP, Init. Repts.,* 193 [CD-ROM]. Available from: Ocean Drilling Program, Texas A&M University, College Station TX 77845-9547, USA.

Taylor, S.R., and McLennan, S.M., 1985. *The Continental Crust: Its Composition and Evolution:* Oxford (Blackwell Scientific).

Von Damm, K.L., 1995. Controls on the chemistry and temporal variability of seafloor hydrothermal fluids. *In* Humphris, S.E., Zierenberg, R.A., Mullineaux, L.S., and Thomson, R.E. (Eds.), *Seafloor Hydrothermal Systems: Physical, Chemical, Biological, and Geological Interactions.* Geophys. Monogr., 91:222–247.

Figure F1. Leg 193 drill sites (stars) and principal hydrothermal deposit types at the PACMANUS hydrothermal field on Pual Ridge, Manus Basin, Papua New Guinea. Isobaths are mbsl.
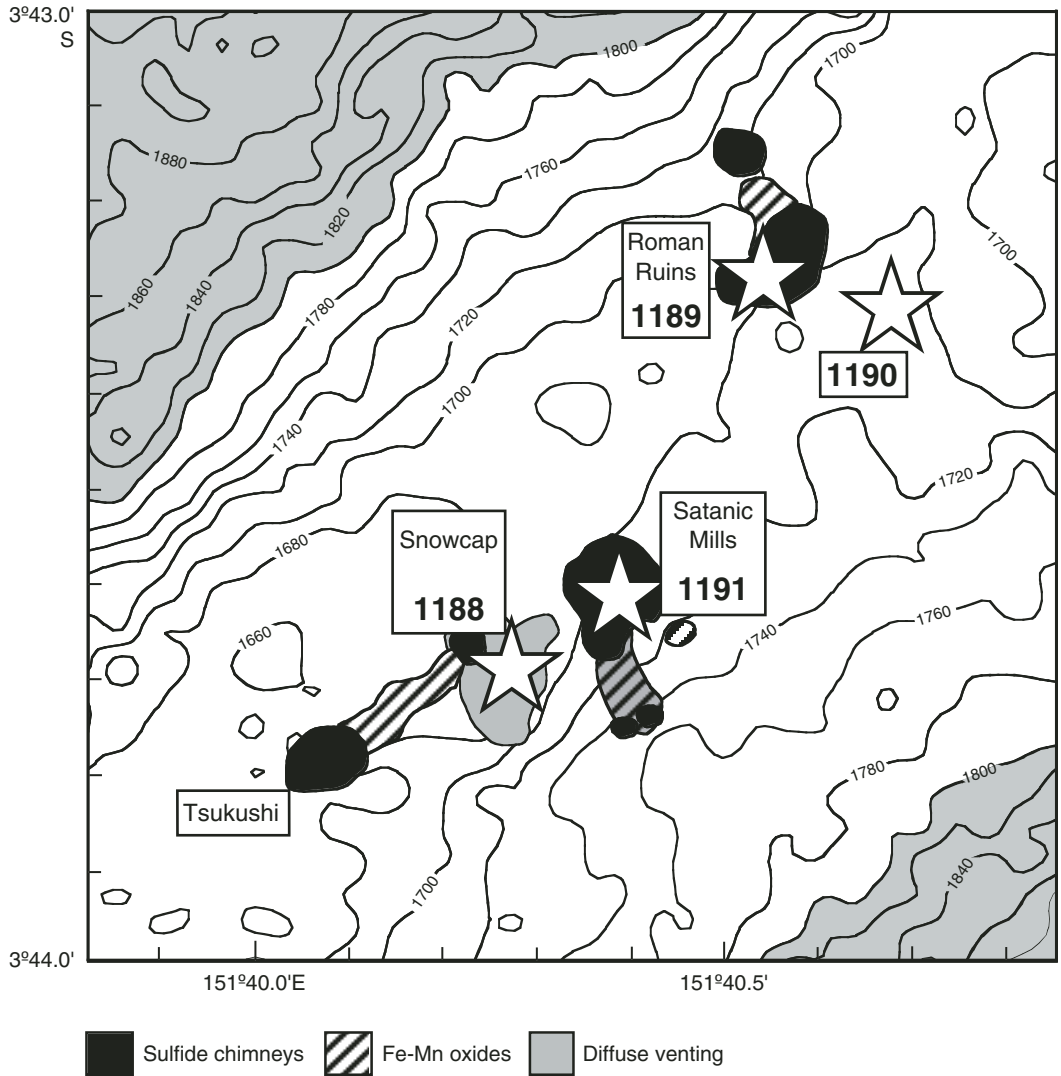
Figure F2. Chondrite-normalized rare earth element profiles for calculated hydrothermal end-members (Mg = 0) of borehole fluids from Holes 1188B and 1189B, of chimney vent fluids at PACMANUS (Table T2, p. 15), and for seawater (Mitra et al., 1994). Chondrite values from Taylor and McLennan, 1985. Numbers in parenthesis = CSIRO numbers.
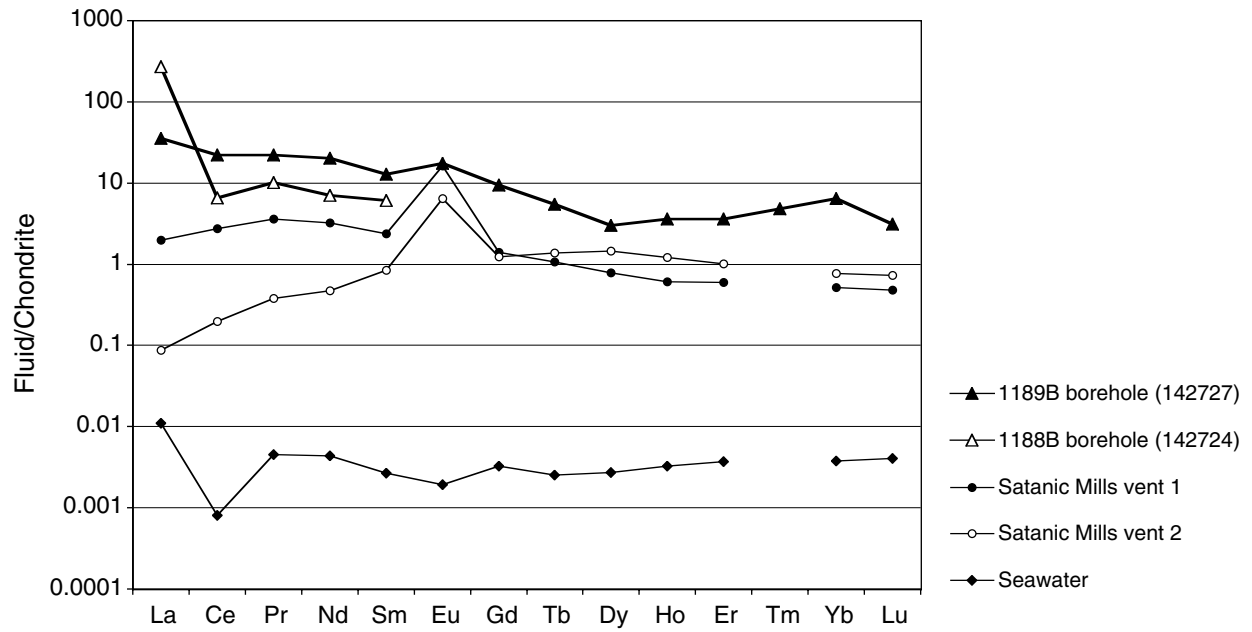
Figure F3. Logarithmic plot of Fe and Mn contents in calculated hydrothermal end-members of borehole fluids from Holes 1188B and 1189B and PACMANUS chimney vent fluids (Table T2, p. 15; data from T. Gammo and C.J. Yeats, pers. comm., 1996 and 2001, respectively). Borehole fluids from Hole 1188 are plotted at 100 times the analyses cited in Table T1, p. 13. Unfiltered fluids collected by vent funnel (VUNL) at Snowcap seeps and by hydrocasts within the PACMANUS plume (1550–1683 mbsl, between Satanic Mills and Roman Ruins) are also plotted for comparison (CSIRO data). Numbers in parenthesis = CSIRO numbers.
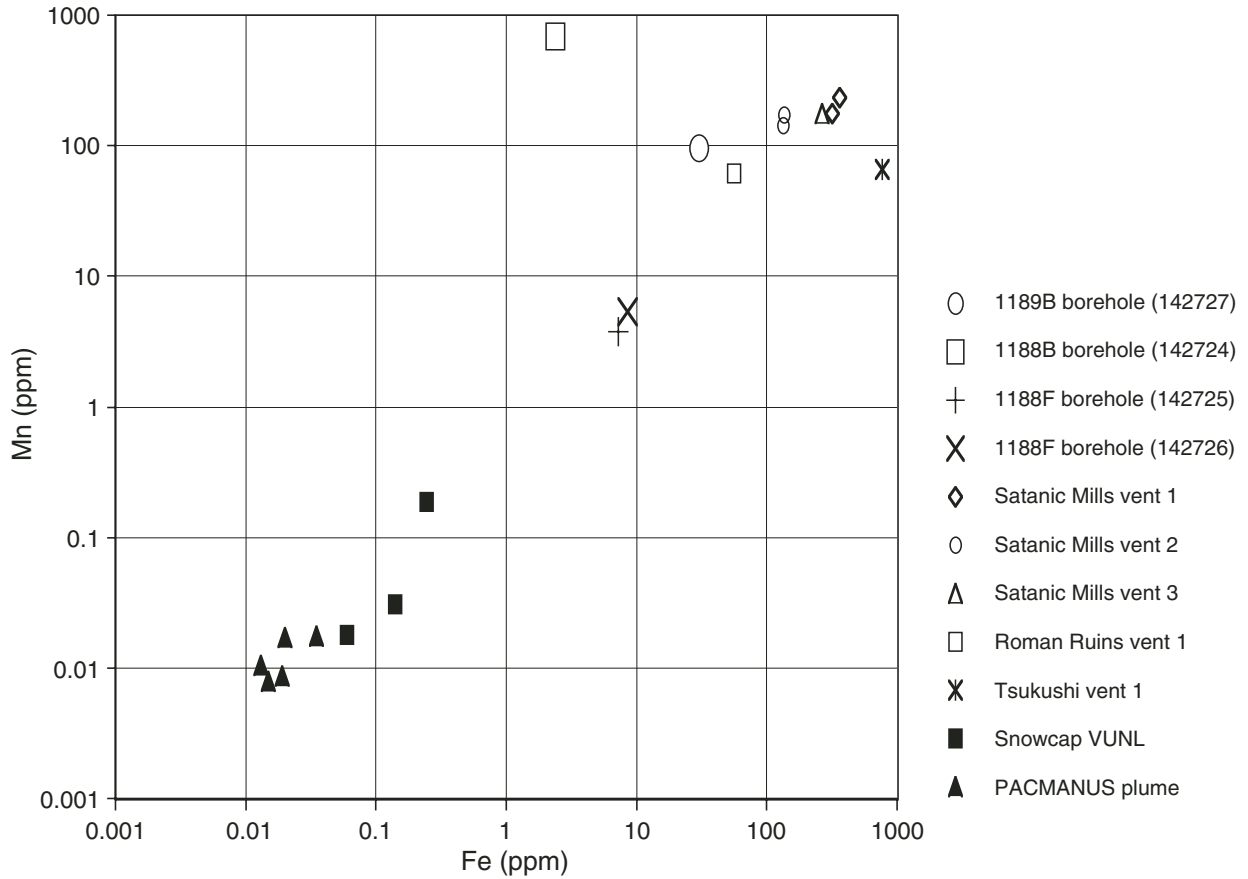
Table T1. Chemistry of filtered borehole fluids and blank samples, Leg 193. (See table notes. Continued on next page.)

Sample	Hole	Depth (mbsf)	Temperature (°C)	Date collected	Rebound time (days)	pH*	Alkalinity* (mM/L)	Salinity* (‰)	$^{87}Sr/^{86}Sr$	2SE (%)
CSIRO Number										
Borehole fluids:										
142724	1188B	3	6	22-Dec-00	25	7.9	2.06	31	0.708989	0.0012
142725	1188F (1)	107	12	27-Dec-00	6	8.0	2.28	34	0.709141	0.0017
142726	1188F (2)	207	21	29-Dec-00	8	7.7	1.91	35	0.709158	0.0012
142727	1189B	130	55	26-Dec-00	1	7.0	2.04	34	0.708270	0.0017

|	Element:	Li	Be	B	Na	Mg	Al	Si	P	S	K	Ca	Sc	Sc
	Method:	ICP–AES	ICP–AES	ICP–AES	ICP–AES	ICP–AES	ICP–AES	ICP–AES	ICP–AES	ICP–AES	ICP–AES	ICP–AES	ICP–AES	ICP–MS
Sample	Unit:	(ppm)	(ppm)	(ppm)	(ppm)	(ppm)	(ppm)	(ppm)	(ppm)	(ppm)	(ppm)	(ppm)	(ppm)	(ppb)
CSIRO Number														
Borehole fluids:														
	DL	0.005	0.002	0.005	0.2	0.01	0.005	0.1	0.05	0.2	0.2	0.01	0.005	2
142724		0.27	ND	3.4	9,711	1,153	0.030	2.5	0.05	911	375	468	0.001	NA
142725		0.20	ND	4.4	10,782	1,279	0.076	3.1	0.03	936	414	429	ND	NA
142726		0.20	ND	4.4	10,792	1,285	0.049	3.1	0.04	932	412	426	0.001	NA
142727		0.85	ND	5.3	10,621	1,124	3.0	42	0.01	1,049	635	756	ND	NA
Blank samples:[†]														
	DL	0.005	0.002	0.005	0.2	0.01	0.005	0.1	0.05	0.2	0.2	0.01	0.005	0.07
142728A		ND	ND	ND	ND	ND	ND	ND	ND	ND	ND	0.01	ND	ND
142728B		ND	ND	ND	ND	ND	ND	ND	ND	0.01	ND	0.02	ND	ND
142728C		ND	ND	ND	ND	0.008	ND	ND	ND	0.01	ND	0.04	ND	ND

	Element:	Ti	V	Cr	Mn	Fe	Co	Co	Ni	Ni	Cu	Zn	Zn	Ga
	Method:	ICP–AES	ICP–AES	ICP–AES	ICP–AES	ICP–AES	ICP–AES	ICP–MS	ICP–AES	ICP–MS	ICP–AES	ICP–AES	ICP–MS	ICP–MS
Sample	Unit:	(ppm)	(ppm)	(ppm)	(ppm)	(ppm)	(ppm)	(ppb)	(ppm)	(ppb)	(ppm)	(ppm)	(ppb)	(ppb)
CSIRO Number														
Borehole fluids:														
	DL	0.005	0.005	0.005	0.002	0.01	0.01	0.1	0.03	0.4	0.005	0.05	2	0.1
142724		0.002	0.004	0.012	15.1	0.056	ND	7.4	0.10	178	0.096	5.5	5,493	0.4
142725		0.001	ND	0.014	0.038	0.072	ND	1.4	0.01	11	0.004	3.4	3,183	0.1
142726		0.002	ND	0.009	0.054	0.085	ND	1.7	0.01	21	0.004	1.6	1,688	0.1
142727		0.024	0.004	0.010	11.9	3.73	0.006	8.7	0.14	256	0.59	1.5	1,664	0.8
Blank samples:														
	DL	0.005	0.005	0.005	0.002	0.01	0.01	0.02	0.03	0.03	0.005	0.05	0.06	0.1
142728A		ND	ND	ND	ND	ND	ND	0.02	ND	0.06	ND	ND	7.1	ND
142728B		ND	ND	ND	0.001	0.01	ND	0.02	ND	0.04	ND	0.03	6.0	ND
142728C		ND	ND	ND	0.001	0.01	ND	0.03	ND	0.82	ND	0.02	12.4	ND

Table T1 (continued).

Sample	Element: Method: Unit:	Ge ICP–MS (ppb)	As ICP–MS (ppb)	Rb ICP–MS (ppb)	Sr ICP–AES (ppm)	Sr ICP–MS (ppb)	Y ICP–MS (ppb)	Mo ICP–AES (ppm)	Mo ICP–MS (ppb)	Cd ICP–AES (ppm)	Cd ICP–MS (ppb)	In ICP–MS (ppb)	Sb ICP–MS (ppb)	Te ICP–MS (ppb)
CSIRO Number Borehole fluids:														
	DL	*0.7*	*4*	*0.1*	*0.002*	*0.2*	*0.07*	*0.01*	*0.3*	*0.01*	*0.1*	*0.2*	*0.2*	*0.4*
142724		ND	NA	112	6.9	OR	0.17	0.25	360	0.06	98	ND	5.1	0.4
142725		ND	NA	110	7.4	OR	0.07	0.01	17	ND	1.3	ND	0.6	ND
142726		ND	NA	110	7.4	OR	0.14	0.01	16	ND	1.0	ND	0.9	ND
142727		2.8	NA	674	9.0	OR	0.87	0.04	71	0.06	109	ND	9.8	0.4
Blank samples:														
	DL	*0.02*	*0.1*	*0.003*	*0.002*	*0.01*	*0.002*	*0.01*	*0.01*	*0.01*	*0.01*	*0.05*	*0.006*	*0.01*
142728A		ND	ND	0.02	ND	0.15	0.007	ND	0.14	ND	0.02	ND	0.031	ND
142728B		ND	ND	0.02	ND	0.09	0.006	ND	0.28	ND	0.04	ND	0.027	ND
142728C		ND	ND	0.02	ND	0.12	0.011	ND	0.08	ND	0.10	ND	0.018	ND

Sample	Element: Method: Unit:	Cs ICP–MS (ppb)	Ba ICP–AES (ppm)	La ICP–MS (ppb)	Ce ICP–MS (ppb)	Pr ICP–MS (ppb)	Nd ICP–MS (ppb)	Sm ICP–MS (ppb)	Eu ICP–MS (ppb)	Gd ICP–MS (ppb)	Tb ICP–MS (ppb)	Dy ICP–MS (ppb)	Ho ICP–MS (ppb)	Er ICP–MS (ppb)
CSIRO Number Borehole fluids:														
	DL	*0.08*	*0.005*	*0.09*	*0.03*	*0.03*	*0.4*	*0.15*	*0.14*	*0.08*	*0.05*	*0.15*	*0.07*	*0.17*
142724		3.0	0.047	2.21	0.14	0.03	0.11	0.18	ND	ND	ND	ND	ND	ND
142725		0.4	ND	0.28	0.07	0.03	ND	ND	ND	ND	ND	ND	ND	ND
142726		0.6	ND	0.25	0.13	ND	ND	ND	ND	ND	ND	ND	ND	ND
142727		33.3	0.26	1.61	2.6	0.38	1.8	0.37	0.19	0.36	0.04	0.14	0.04	0.11
Blank samples:														
	DL	*0.06*	*0.005*	*0.006*	*0.004*	*0.002*	*0.001*	*0.015*	*0.008*	*0.007*	*0.02*	*0.001*	*0.005*	*0.003*
142728A		ND	ND	0.09	0.013	0.009	0.008	ND	0.010	ND	0.007	0.004	0.007	0.004
142728B		ND	ND	0.10	0.031	0.010	0.009	ND	0.010	0.005	0.008	0.001	0.007	ND
142728C		ND	ND	0.13	0.017	0.006	0.006	ND	ND	ND	ND	0.004	0.004	ND

Sample	Element: Method: Unit:	Tm ICP–MS (ppb)	Yb ICP–MS (ppb)	Lu ICP–MS (ppb)	Tl ICP–MS (ppb)	Pb ICP–MS (ppb)	Bi ICP–MS (ppb)	Th ICP–MS (ppb)	U ICP–MS (ppb)
CSIRO Number Borehole fluids:									
	DL	*0.04*	*0.22*	*0.06*	*0.18*	*0.3*	*0.14*	*0.05*	*0.02*
142724		ND	ND	ND	0.34	6.5	0.20	0.43	1.6
142725		ND	ND	ND	ND	3.7	ND	0.15	3.2
142726		ND	ND	ND	ND	4.0	1.3	0.18	3.5
142727		0.02	0.20	0.01	5.0	38	0.32	0.16	0.89
Blank samples:									
	DL	*0.006*	*0.001*	*0.008*	*0.005*	*0.01*	*0.003*	*0.003*	*0.003*
142728A		0.007	0.007	0.007	0.006	0.28	0.11	0.003	0.008
142728B		0.007	0.007	0.008	0.008	0.28	0.05	0.005	0.006
142728C		0.004	0.005	0.006	0.004	0.26	0.07	0.003	0.007

Notes: * = Shipboard measurement (Binns, Barriga, Miller, et al., 2002). † = blank samples are composed of deionized water acidified as for borehole samples. DL = instrumental detection limit (in italics). ICP–AES = inductively coupled plasma–atomic emission spectroscopy, ICP–MS = inductively coupled plasma–mass spectroscopy, ND = not detected, NA = not analyzed, OR = over instrument range.

Table T2. Components and end-member compositions (Mg = 0) of Leg 193 borehole fluids and PACMANUS chimney vent fluids.

Sample	Components (%)			Calculated end-member $^{87}Sr/^{86}Sr$	Li (ppm)	B (ppm)	Na (ppm)	Mg (ppm)	Al (ppm)	Si (ppm)
	SW	DW	HEM							
Hole 1188B (142724)	89.8	8.0	2.2	0.70642	4.2		12,081	0	1	–11
Hole 1189B (142727)	87.6		12.4	0.70619	5.4	10.3*	11,398	0	24	322
Satanic Mills vent 1 (301-3)†	36.2		63.8	0.70500	6.4		12,124	0	277	439
Satanic Mills vent 2 (301-7)†	41.1		58.9	0.70537	5.2		10,346	0	254	456
Pual Ridge seawater‡				0.70916	0.2	4.6	10,513	1,283	0.003	3

Sample	P (ppm)	S (ppm)	K (ppm)	Ca (ppm)	Ti (ppm)	V (ppm)	Cr (ppm)	Mn (ppm)	Fe (ppm)	Co (ppb)	Ni (ppb)	Cu (ppm)
Hole 1188B (142724)	1.2*	2,084	38*	3,558		0.09*	0.44*	686	2.4	336	8,077	4.4
Hole 1189B (142727)		1,659	2,175	3,030	0.19	0.01*	0.06*	96	30	70	2,062	4.7
Satanic Mills vent 1 (301-3)†		146	4,077	583				232	363			2.5
Satanic Mills vent 2 (301-7)†		138	3,348	410				172	135			2.3
Pual Ridge seawater‡	0.03	962.5	417	434	0.0006	0.003	0.002	0.0002	0.004	0.007	0.3	0.00006

Sample	Zn (ppm)	Ga (ppb)	Ge (ppb)	As (ppb)	Rb (ppb)	Sr (ppm)	Y (ppb)	Mo (ppb)	Cd (ppb)	In (ppb)	Sb (ppb)	Te (ppb)
Hole 1188B (142724)	250	18*			442*	20.4	3.6*	15,894	4,451		218	18*
Hole 1189B (142727)	13	6	23		4,627	21.4	6.3	491	878		77	3*
Satanic Mills vent 1 (301-3)†	15			2,171	7,972	10.2	1.4	9,917	32	8	36	
Satanic Mills vent 2 (301-7)†	8			2,047	6,453	8.8	2.6	3,088	72	20	22	
Pual Ridge seawater‡	0.0002				114	7.2	0.1	12	0.08	0.01	0.3	

Sample	Cs (ppb)	Ba (ppm)	La (ppb)	Ce (ppb)	Pr (ppb)	Nd (ppb)	Sm (ppb)	Eu (ppb)	Gd (ppb)	Tb (ppb)	Dy (ppb)	Ho (ppb)
Hole 1188B (142724)	124	2.1	100.1	6	1.4	5.0	1.4*					
Hole 1189B (142727)	266	2.1	13.0	21	3.1	14.4	3.0	1.5	2.9	0.32	1.1	0.31
Satanic Mills vent 1 (301-3)†	387	12.5	0.729	2.61	0.493	2.28	0.546	1.42	0.426	0.622	0.3	0.0515
Satanic Mills vent 2 (301-7)†	318	0.42	0.0319	0.189	0.052	0.336	0.195	0.557	0.379	0.793	0.548	0.104
Pual Ridge seawater‡	0.31	0.02	0.0040	0.00077	0.00062	0.00309	0.00062	0.00017	0.00099	0.00015	0.00104	

Sample	Er (ppb)	Tm (ppb)	Yb (ppb)	Lu (ppb)	Tl (ppb)	Pb (ppb)	Bi (ppb)	Th (ppb)	U (ppb)
Hole 1188B (142724)					15	294	5.4*	19*	–46
Hole 1189B (142727)	0.90	0.17	1.59	0.12*	40	306	1.9*	1.2*	–13
Satanic Mills vent 1 (301-3)†	0.149		0.127	0.0183	50	1,471			
Satanic Mills vent 2 (301-7)†	0.253		0.190	0.0278	62	1,460			
Pual Ridge seawater‡	0.00092		0.00093	0.00015	0.01	0.03	0.09	0.01	2.9

Notes: SW = seawater calculated from Mg, DW = deionized water estimated from Na (see text), HEM = hydrothermal end-member component by difference. * = estimates subject to greater error. † = recalculated from Douville (1999). ‡ = CSIRO data from hydrocasts outside the PACMANUS plume; italics denote data from Mitra et al. (1994) and assumed $^{87}Sr/^{86}Sr$.